

FINITE SEISMIC SOURCE PARAMETERS INFERRED FROM STOPPING PHASES FOR SELECTED EVENTS OF WEST BOHEMIA 2000 SWARM

Petr KOLÁŘ * and Bohuslav RŮŽEK

Institute of Geophysics, Academy of Sci. of the Czech Rep., Boční II/1401, 141 31 Praha 4, Czech Republic
**Corresponding author's e-mail: kolar@ig.cas.cz*

(Received January 2012, accepted August 2012)

ABSTRACT

Parameters of finite seismic source model were determined for a set of 36 selected events of the West Bohemia 2000 earthquakes swarm (MI from 1.7 to 3.0) using stopping phases method. Two stopping phases are generated along the source border where the rupture process terminates and these phases form Hilbert transform pair, which is also the criterion for their identification. Circular and elliptical source models were considered and corresponding source parameters were calculated by inverting interpreted stopping phases delays. As generalization of circular to elliptical model was found to be statistically insignificant, only results related to the circular source including error estimates are presented. Our results are in a good agreement with previously published theoretical formula concerning source radius and magnitude and also fairly well confirm general theoretical assumption about constant stress drop. The determined stress drop ranges between 1 – 10 MPa with the typical value of 2.4 MPa.

KEYWORDS: finite seismic source, stopping phases, West Bohemia earthquake swarm

1. INTRODUCTION

Study of the seismic source plays permanently an important role in geophysics. The theory of the earthquake seismic source has a long history (for a comprehensive overview see e.g. Aki and Richards, 1980): starting with simple models imitating point source (first with dipole and later on with double-couple mechanism – see e.g. Lay and Wallace, 1995), through more general mathematical formalism using the notion of seismic moment tensor and enabling to describe more complex point sources (ibid.), and terminating with complex composite models of seismic source of finite size or higher order seismic moment tensor formalism (e.g. Adamová and Šílený, 2010). While the theory of seismic source may be practically indefinitely complex, real measurements depend on many other circumstances, which are commonly difficult to take fully into account (e.g. velocity model of the medium). Therefore some simplification and parameterization is always necessary.

As concerns finite seismic source, first models were based on simple assumptions on the rupture geometry and the rupture dynamics (e.g. Brune, 1970; Madariaga, 1976; Boatwright, 1980). Since then, detailed structure of large world earthquakes has been studied for tens of years and such big events are now processed in some sense more or less routinely (e.g. Ihmlé and Ruegg, 1997). There is also an alternative to this “deterministic” approach: a “stochastic”

approach, when agreement of some important earthquake features is required (usually shape of the spectrum, fit of the maximum amplitudes, etc.) for observed data and stochastic model – see e.g. Beresnev and Atkinson (1998), Plicka and Zahradník (2002).

Quantitative and qualitative development of observations achieved during last years enabled application of the above mentioned techniques to smaller events. This is also the case of the West Bohemia events. Seismic activity in the West Bohemia region (hereafter W.B.) is definitely the most important seismic phenomenon on the territory of the Czech Republic. The activity is characterized by the occurrence of seismic swarms (Horálek et al., 2009; Fischer et al., 2010; wwwWEBNET, 2012). The seismic activity is not only continuously monitored (the most important role plays data recorded by seismic network WEBNET, however various sorts of physical values are observed – see e.g. Kolář et al., 2010), but it is also subject of numerous studies which investigated it from all sorts of points: see e.g. special issues of *Studia Geoph. and Geod.* (2000, 2008, 2009) or the most recently published works – e.g. Gaždová et al. (2011), Schenk and Schenková (2011), Štrunc and Brož (2011).

We determined parameters of finite circular or elliptical seismic source respectively, for a set of 36 selected events from W.B. 2000 swarm by using “stopping phases” method. The method is not quite

new (the “stopping phase” term can be traced back for several decades), however, it has never become a routine method. It is particularly designed for application to weaker earthquakes which are generally believed to be well approximated by circular source model and which is also the case of W.B. earthquakes.

2. METHOD

Stopping phases method is based on a relatively simple idea. Finite seismic source is modelled as a rupture propagating radially from a nucleation point along the fault plane until reaching boundary defining source dimensions (in our model the boundary is supposed to be of circular or elliptical shapes, respectively). For such a rupture process, three phases can be identified in seismograms, both for P and S waves: (i) first arrival phase, which corresponds to the beginning of the rupture process (i.e. radiation from the nucleation point), and (ii) two stopping phases, which correspond to stopping points situated on the edge of the ruptured source area. In a figurative way, the stopping phases can be linked to abrupt changes of observed displacement produced by a finite source. When the rupture process reaches the source boundary and fades in a particular direction, such a change results in a change of slope of displacement pulse, which can be (in twice differentiate displacement signal, i.e. in accelerogram) interpreted as a stopping phase. Imanishi and Takeo (1998, 2002) proposed, based on the theory derived by Bernard and Madariaga (1984), a methodology for stopping phases identification and their inversion for finite source parameters determination: the two stopping phases are in mutual relation as a pulse and its Hilbert transform, which is also the criterion for their identification. The time lags between these phases depend on source size, geometrical orientation of the finite source and on the mutual position of the source and a station. Therefore first we have to search for the stopping phases in seismograms. The time delays between onset and these two stopping phases represent the input data, which are subject of inversion. The finite source itself is represented either as a circular or an elliptical model. Circular source model is often used for modelling of moderate events as it is the case of the W.B. earthquakes. The elliptic source can be easily converted into circular or linear one. In case of circular source there are only two parameters to be determined during the inversion: source radius and rupture velocity. All other required information, i.e. position of the source and the fault orientation and velocity model of the medium, which are necessary for forward problem modelling, are supposed to be known from earlier studies.

The circular source model is described by its radius and rupture velocity. In case of extension of the model to elliptic source four parameters are to be determined: size of the half-axis of the ellipse (instead of circular source radius), its eccentricity, its orientation on the fault plane and rupture velocity.

Values of these parameters have to be determined during inversion to fit stop phases arrivals as well as possible.

Since the whole stopping phase method is rigorously described in Imanishi and Takeo (1998, 2002), only final formulas directly used in evaluating the forward problem will be given here. The distance r from a fault plane point is (Eq. 2 in Imanishi and Takeo, 2002)

$$r(\xi, \phi') = \sqrt{\xi^2 + r_0^2 - 2\xi r_0 \sin \theta \cos(\phi - \phi')}, \quad (1)$$

(meaning of symbols is shown in Fig. 1). The circular/elliptical source barrier ξ_b , where all the rupture process stops, is given as (ibid. Eq. 5, see Fig. 2.) $\xi_b(\phi') = a(1 - \varepsilon^2)/(1 - \varepsilon \cos \phi')$, for $0 \leq \varepsilon \leq 1$, where $\varepsilon = \sqrt{1 - (b/a)^2}$ is the eccentricity of an ellipse with minor and major half-axes b and a , resp. Then final equation relating all required values is given by (ibid. Eq. 6):

$$\frac{c}{v_s v_r} = \frac{r_0}{r[\xi_b(\phi'); \phi']} \left\{ \frac{\sin \theta \left[\sin \phi + \frac{\sin(\phi' - \phi)}{\varepsilon} \right] - \frac{\xi_b(\phi')}{r_0}}{\sin \phi'} \right\} \quad (2)$$

where c is the P or S waves velocity and v_r is a dimensionless fracture of v_s velocity – rupture velocity is conventionally often given in such a form. As follows from the theory, there are two particular values of $\phi'_{cr1,2}$ angle (“critical angles”) which defines “critical points” on the source barrier from

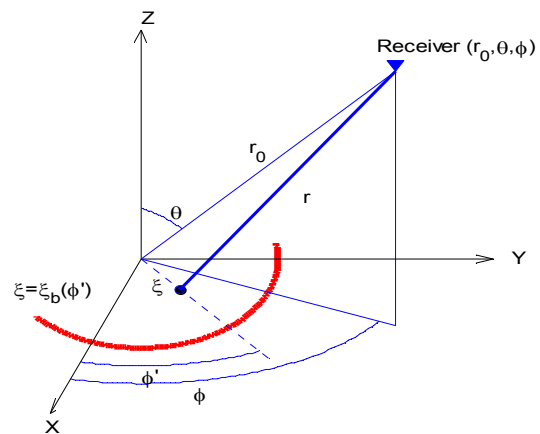


Fig. 1 Coordinate system and notation used in this study. The fault is situated in the x - y plane. A point of the fault is described by distance ξ and angle ϕ' , with distance r to the receiver point (r_0, θ, ϕ) . The bold line $[\xi_b(\phi')]$ represents part of the barrier line where the rupture terminates – adopted from Imanishi and Takeo (2002).

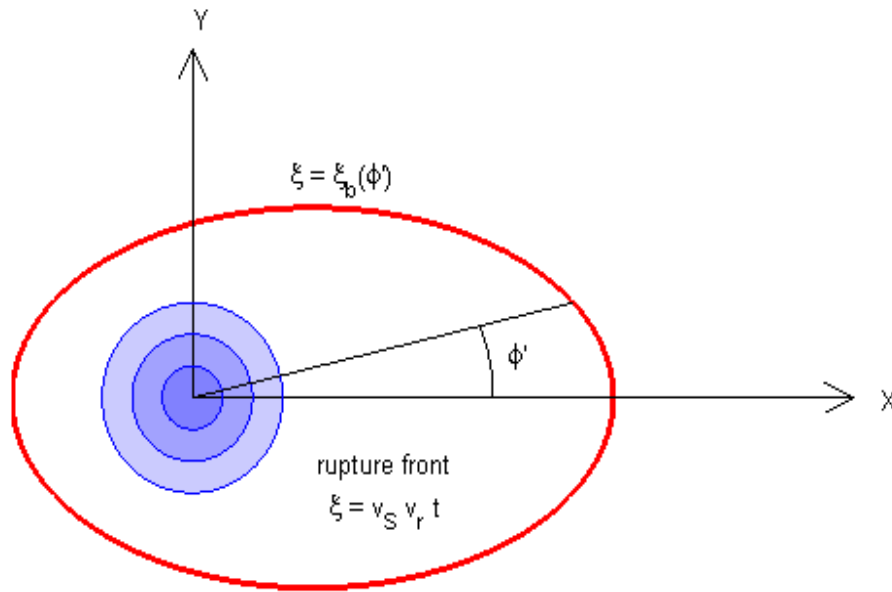


Fig. 2 An elliptical fault model; the rupture starts in one focus of an ellipse fault and spreads circularly with a constant rupture velocity $v_s v_r$. The shaded area shows a region over which faulting has already occurred – adopted from Imanishi and Takeo (2002).

which the stopping phases are generated. Imanishi and Takeo (1998) declared that there is no analytical solution to Equation 2; this fact was also proved by our attempt using Matlab Symbolic Toolbox. Therefore we use iterative bisection approach. For circular source model the “critical points” correspond to the closer and the farther points of the source (observed from a station), e.g. critical angle is identical with station azimuth ϕ and its complementary value which is shifted by $\pm 180^\circ$.

Our task was to find values of 2 or 4 parameters describing circular or elliptical source model. We accomplished it by using the algorithm designed by Boender et al. (1982) and Czendes (1988), wwwBRST (2012). During the inversion we required minimization of the squared difference between observed stopping phases delays $\Delta T_{c1,2} = T_{c1,2} - T_{c0}$, where T_{c0} is P or S waves onset and $T_{c1,2}$ interpreted arrivals of stopping phases and the same values calculated for a model $\Delta t_{c1,2} = t_{c1,2} - t_0$, where t_0 is the theoretical P or S waves first onset and $t_{c1,2}$ are arrivals of corresponding stopping phases. The $t_{c1,2}$ times are given as

$$t_{c1,2} = \frac{\xi_b(\phi'_{cr1,2})}{v_s v_r} + \frac{r[\xi_b(\phi'_{cr1,2}); \phi'_{cr1,2}]}{c}, \quad (3)$$

where the first term represents time of rupture propagation from the hypocentre to the critical point and the second one represents propagation of the wave

generated in these points to the station. Consequently, for each tested model, the values of critical angles $\phi'_{cr1,2}$ have to be determined with use the of (2). In extension to the work of Imanishi and Takeo (2002), where the orientation of elliptical source is searched for ex post separately, we incorporated this parameter directly into inversion. The numerical code was successfully tested using synthetic data generated for the same geometrical configuration as it is valid for the real data.

3. DATA

We processed data from the West Bohemia earthquake swarm which occurred during year 2000 (see Fig. 3). The swarm lasted approximately from August to December, $M_{I_{max}}=3.3$, and about 4000 events with $M_I > 0$ were recorded and located by using automated method (Fischer, 2003). Unfortunately, the final number of events suitable for source inversion reduced to only 36 events. The most limiting factor was the necessity concerning the knowledge of the source mechanisms, which were available only for a small fraction of the stronger events.

We used the subset of data processed by Fischer (2005), their locations were obtained from Webnet catalogue (wwwWEBNET, 2012), see Table 1.

4. DATA PROCESSING

Generally, the data were processed in a way similar to procedure given in Imanishi and Takeo

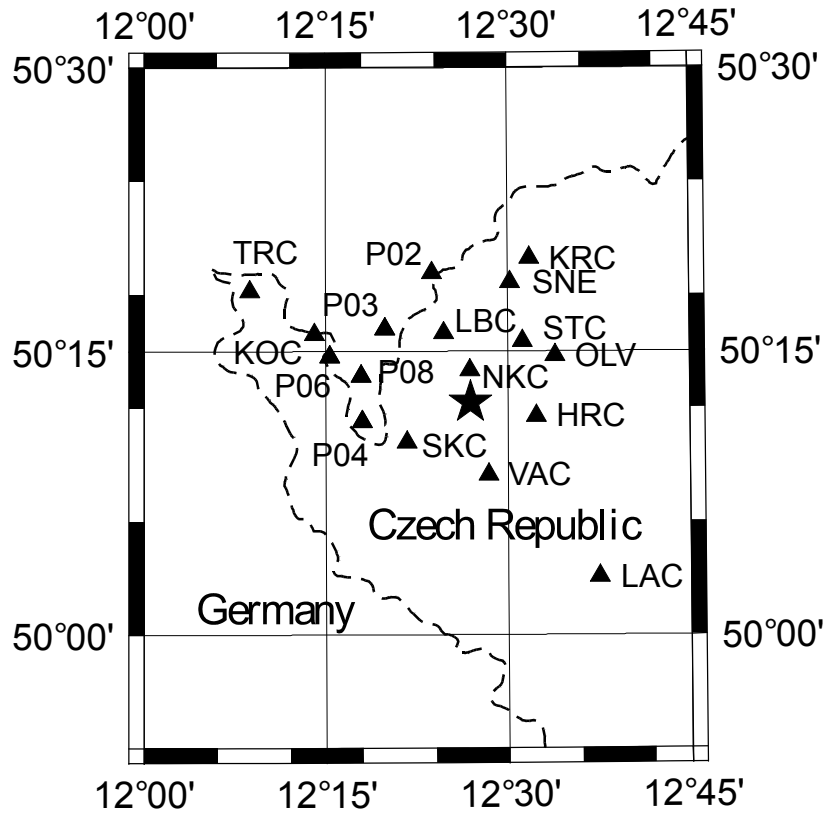


Fig. 3a Position of used stations (triangles) and area of epicentres of processed events (a star southerly from station Nový Kostel – NKC).

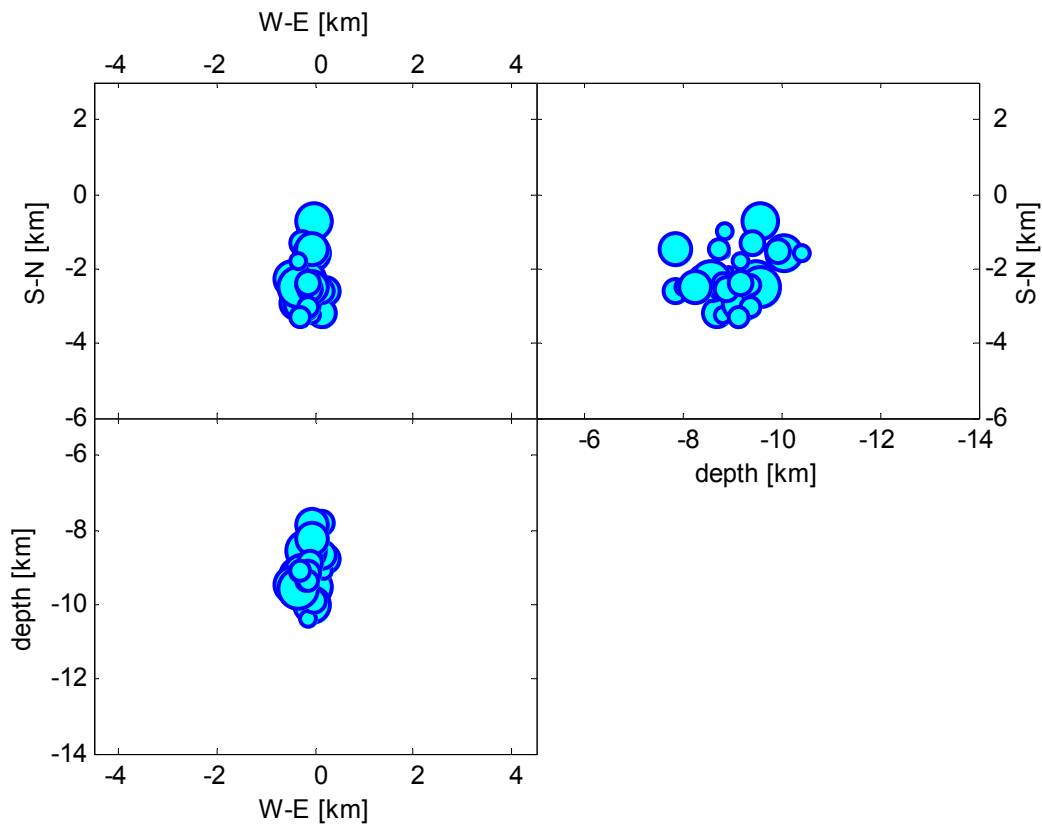


Fig. 3b Detailed distribution of hypocenters of investigated events. Upper left subplot is a horizontal projection, upper right subplot is projection on a vertical plane oriented in NS direction seen from E, lower subplot is a projection in a vertical plane oriented in WE direction seen from S. The distances are measured in [km] from station NKC, the sizes of circles are scaled according event magnitudes, only processed events are plotted.

Table 1 List of processed events.

Particular columns include event number No., event identification (according to WEBNET database system), date and time of event origin, magnitude M_l , epicentre coordinates in [m] relatively to the station Nový Kostel (NKC, coordinates: N50.2331, E12.4479, altitude: 564 m) and source mechanism [dgr].

No.	Event. Id	YYYY-MM-DD	hh:mm:ss	M_l	EW	NS	depth	strike	dip	rake
1	P1480A	2000-09-04	00:16:35	2.0	-178	-965	-8830	-11	79	44
2	P1493A	2000-09-04	00:31:45	2.8	-18	-743	-9550	-16	90	40
3	P1562A	2000-09-04	01:51:43	2.3	-269	-1299	-9400	196	79	-49
4	P2260A	2000-09-08	11:39:50	2.8	-69	-1580	-10030	1	85	30
5	P2278A	2000-09-08	12:00:15	2.0	-133	-1570	-10400	-9	90	35
6	P2483A	2000-09-08	18:35:48	2.4	-6	-1501	-9910	167	76	-27
7	P3001A	2000-09-17	09:45:01	1.8	179	-1565	-8840	161	73	-31
8	P3265A	2000-09-17	14:52:33	2.2	-182	-1472	-8700	171	84	-35
9	P3887A	2000-10-15	19:11:20	2.5	240	-2600	-8780	175	81	-34
10	P3927A	2000-10-15	19:58:51	2.1	165	-3366	-9110	3	79	44
11	P3930A	2000-10-15	20:03:00	2.5	132	-3169	-8680	5	87	20
12	P4085A	2000-10-16	09:46:39	2.4	-156	-2546	-8990	172	78	-22
13	P4270A	2000-10-16	17:56:11	2.3	141	-2584	-7830	159	50	-23
14	P4277A	2000-10-16	18:01:38	2.0	-72	-2166	-8310	170	59	-16
15	P4342A	2000-10-16	19:57:08	1.7	-186	-2068	-8930	163	67	-63
16	P4502A	2000-10-17	13:23:02	2.1	78	-2484	-8010	155	54	-59
17	P4548A	2000-10-17	14:26:14	2.2	-159	-2478	-8190	164	48	-48
18	P4621A	2000-10-17	22:45:32	2.2	29	-2430	-8350	180	83	-45
19	P4744A	2000-10-23	21:22:01	2.9	-169	-2319	-8550	165	56	10
20	P4845A	2000-10-24	01:35:41	2.0	-172	-2510	-8970	166	71	-30
21	P4846A	2000-10-24	01:36:35	1.9	-189	-2395	-8940	166	67	-20
22	P4888A	2000-10-24	03:19:55	2.2	-120	-2372	-8790	162	63	-14
23	P5036A	2000-10-26	01:35:52	2.1	-37	-2611	-8710	178	80	-28
24	P5164A	2000-10-29	05:10:47	2.6	-72	-1467	-7850	155	55	-45
25	P5395A	2000-11-06	20:59:55	2.1	-43	-3219	-8810	166	66	-33
26	P5410A	2000-11-06	21:10:18	2.6	-401	-2934	-9220	167	66	-26
27	P5500A	2000-11-06	22:34:37	2.8	-258	-2902	-9150	161	69	-22
28	P5515A	2000-11-06	22:50:36	2.7	-68	-2493	-8240	176	80	-39
29	P5562A	2000-11-06	23:34:25	2.8	-448	-2296	-9480	175	82	-18
30	P5581A	2000-11-06	23:53:07	3.0	-322	-2497	-9570	166	73	-10
31	P5839A	2000-11-07	14:17:02	2.1	-340	-1772	-9170	158	66	-33
32	P5892A	2000-11-07	17:06:22	2.2	-191	-2451	-9350	175	71	-30
33	P5964A	2000-11-07	19:12:09	2.3	-109	-2566	-8890	166	67	-20
34	P6056A	2000-11-07	21:29:13	2.4	-157	-2377	-9160	183	83	-29
35	P6066A	2000-11-07	21:40:46	2.2	-125	-3014	-9360	157	71	-36
36	P6260A	2000-11-08	02:13:54	2.2	-309	-3299	-9100	176	71	-24

(1998, 2002). Stopping phases were only identified by using SH waves. Therefore selected parts of seismograms were first rotated into ZRT system, then filtered (band-pass filter 15-85 Hz was used, but the upper limit is rather formal – the high-pass filter could be used with the same effect). Then the signal was differentiated (to obtain accelerograms from original velocigrams) and finally the Hilbert transforms of these signals were calculated. If f_{c1} and f_{c2} are waveforms corresponding to the first and the second stopping phases, resp., then their Hilbert transform

fulfil the relation $H[f_{c1}] = f_{c2}$ and $H[f_{c2}] = -f_{c1}$ (Imanishi and Takeo, 1998, 2002). Based on these relations, the stopping phases positions are searched for in the time domain as maximal mutual correlation of signals (accelerograms) and their Hilbert transforms.

Originally Imanishi and Takeo (1998, 2002) used only the SH waves and they declared that using of the P waves (Z component) was inconvenient due to low P amplitudes and their unclear interpretation. In our case, the P waves are fairly clear and we tried to use them as well. However, the cross-correlation

diagrams were so messy (numerous local maxima without single distinguished global maximum of correlation) that the positions of stopping phases could not be interpreted. Cross-correlation of the SH waves were much clearer, having only few maxima and the position of stopping phases could be picked automatically in many cases.

The stopping phases interpretation appeared to be the most crucial part of the work. In some cases, the used waveforms are more complex (probably influence of complex medium structure and/or more complex source mechanism), that there are dominant maxima with unrealistic positions of stopping phases in cross-correlation diagrams (level of correlation plotted as function of values of two stopping phases onsets). We interpreted individual events and individual stations interactively in order to avoid potential artefacts caused by irregularities of particular signals. We created a (semi)interactive tool (based on MATLAB platform) to effectively handle the stopping phases interpretation together with their consequent inversion (Kolář, 2011). The example of stopping phases interpretation is given in Figure 4. In case that automatically picked stopping phase position obviously unrealistic and simultaneously there was a pronounced secondary maximum closer to its expected theoretical position, we interactively selected the more realistic values as stopping phases interpretation. The same approach was used by Imanishi et al. (2004).

The inversion was performed by Boender's method (Boender et al., 1982; Csendes, 1988; wwwBRST, 2012). This method integrates random global search and local linear search for finding the misfit minimum. It is also capable to determine multiple local minima; our final solution is then that having the lowest misfit. Common L2 norm evaluated as a sum of squared of differences between observed and synthetic data was defined as the misfit. The method does not require any starting model (generally, the population of starting models is generated randomly) but a suitable starting model can be included into the set of starting models if available. The range of inverted parameters is limited according to their physical nature: e.g. we allowed relative rupture velocity v_r to vary in the interval from 0.4 to 1.0 of the S wave propagation velocity v_s . As starting values of source radius we used an estimation based on the theoretical model. We put starting value of eccentricity ε to zero in case of elliptical source model inversion to ensure that circular source solution is incorporated into set of considered models and cannot be accidentally missed during random part of inversion process. Such approach made the calculations faster and the convergence more robust.

As opposed to Imanishi et al. (2004) we did not consider both possible fault plane solutions. We have processed only one fault plane solution per event adopted from previous studies.

5. INVERSION

5.1. CIRCULAR SOURCE INVERSION

Forward modelling was performed for simple velocity model: a homogeneous half-space with $v_p=6.5$ km/s, $v_s=3.94$ km/s, ($v_p/v_s=1.65$). A more complex 1D model (a low velocity layer over a gradient half-space) was optionally tested, but numerical tests showed only insignificant differences.

In the first step we supposed circular source model; i.e. we were looking for circular source radius and rupture velocity during the inversion. The results of this type of inversion are given in Table 2. Unfortunately coupling between inverted parameters appeared in some cases: higher value of rupture velocity can be compensated by bigger source radius and vice versa. Our inversions were sufficiently over-determined (readings from 6 station, i.e. 12 time values were available per event on average – Fig. 5), but the azimuthal coverage of the seismic stations currently included into inversion was rather unfavourable. This fact is illustrated in Figure 4b, from where unfavourable azimuthal coverage (especially in S and SW directions) is well visible. WEBNET network configuration was designed with respect to geological structure of the area (e.g. seismograms of reasonable quality cannot be recorded in sedimentary basins which extends southwards from the Nový Kostel (NKC) station) and, consequently not all ray azimuths are always accessible. Therefore we decided optionally to fix the rupture velocity to the value of $0.85 v_s$, i.e. to the average value from previous inversions, which is also close to the frequently referenced value of $0.9 v_s$. Using such simplification, some extreme values of determined parameters obtained without the fixation were eliminated.

Standard Jack-knife method (Tichlaar and Ruff, 1989; Rao and Shao, 1992) was used for estimating the errors of searched parameters. Note that due to stochastic nature of the inversion algorithm, both results and their errors can slightly vary if inversion was repeated; nevertheless fairly stable results were achieved.

5.2. ELLIPTICAL SOURCE INVERSION

We used also elliptical source model in inversions, i.e. we searched for the size of major half-axis a , rupture velocity v_r , eccentricity ε and orientation of the source in the fault plane characterized by angle α . Similarly as above due to coupling between size of the half-axis a and rupture velocity v_r , we optionally fixed the rupture velocity and repeated the inversions.

Elliptic source represents more complex model compared to the circular one and consequently fits the data better. We checked how much is the improvement of the fit statistically significant: we performed standard F-test (Press et al., 1992; Menke, 1989) – i.e. we tested the ratio $F=(\chi_1)^2/(\chi_2)^2$, where

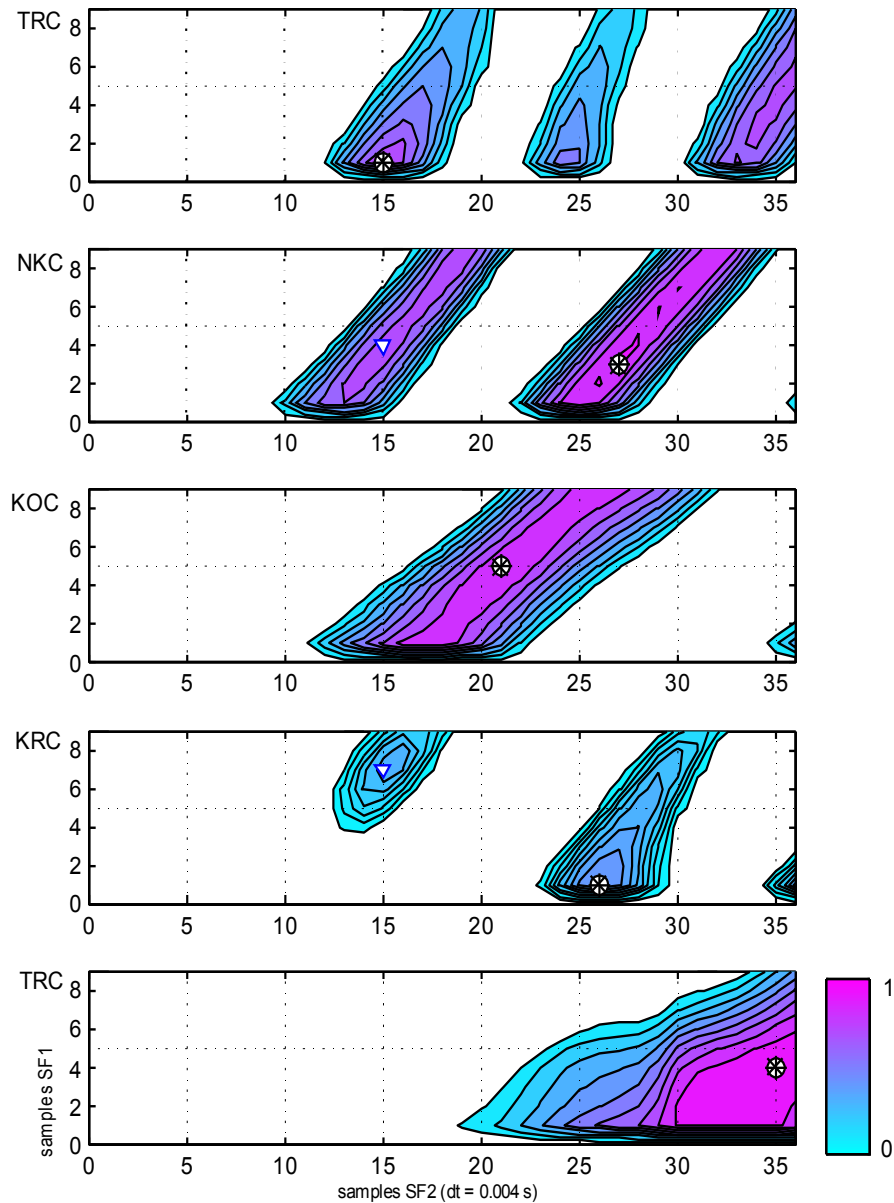


Fig. 4a An example of stopping phases interpretation. Values of mutual correlation pattern of signals and their Hilbert transforms are plotted for investigated stations (for event No. 1). The scales are given in seismogram samples measured from S wave onset. The 1st stopping phase onset is on vertical axes, the 2nd one on horizontal axes). Correlation maxima are marked by circles. The interpretation of stopping phases for stations NKC and KRC are shifted to secondary maxima (marked by triangles) which positions are more realistic; the station LAC is excluded from the processing. Even if the absolute value of correlation for station KRC is not too high (it is less than 0.5, which was generally required minimum level), we decided to keep this station in the inverted data set (removal of this data would make the coverage even worse than it is now – see Fig. 4b).

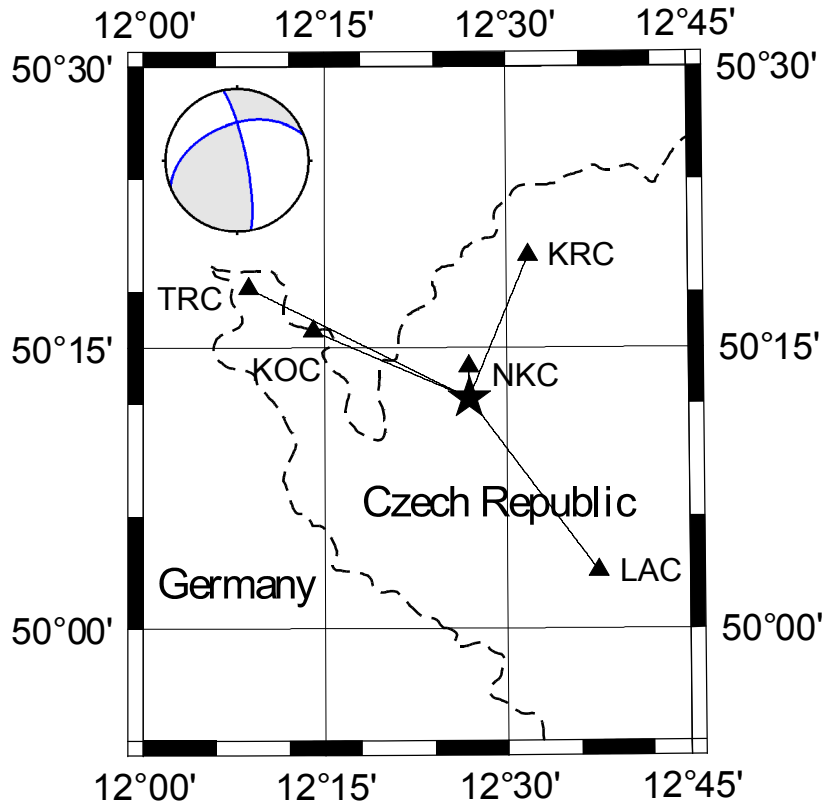


Fig. 4b Azimuthal distribution of stations used for inversion – an example of event No. 1. Station LAC had to be excluded due to unrealistic stopping phases positions; we keep station KRC in the inversion despite of not too high value of correlation, to preserve at least certain level of azimuthal coverage of the investigated event. Unfortunately, azimuthal differences between stations TRC and KOC and between stations KRC and NKC are not too high. Focal mechanism of processed event is plotted as well.

$(\chi)^2 = 1/v \sum_i e_i^2 / \sigma_i^2$, where $i=1,2,\dots,N$; $v=N-M$; e is the difference between data and model, σ is observation error, N is number of data and M is number of inverted parameters, $(\chi_1)^2$ is value for circular source model, i.e. $M=2$ and $(\chi_2)^2$ for the extended elliptical source model, i.e. $M=4$. We suppose uniform data error σ as the individual errors are not known; then the F-value is independent on σ . The particular values of F were taken from Miller (1989); similar application of F-test was also used in Kolář (2003).

The step from circular to elliptical source is not statistically significant based on F-test. There are two possible explanation: (i) the circular source model is fairly good approximation in our case or (ii) the elliptical source model parameters cannot be determined with sufficient accuracy due to unfavourable stations configuration. Due to statistical insignificance of extended elliptical model, we do not present here particular results.

5.3. INTERPRETATION OF RESULTS

In addition to the directly inverted parameters, we determined coefficients in formula relating M_l and

source radius r in the form of $r = C_1 * 10^{(C_2 * M_l)}$ – we were searching for the coefficients of the best fitting curve. Such relation was studied by Fischer and Horálek (2005) by combining the relation for seismic moment $M_0 = (16/7)r^3 \Delta\sigma$ ($\Delta\sigma$ stands for stress drop, see e.g. Stein and Wyssession, 2003) with empirical relation between magnitude and seismic moment for the area of the interest $\log M_0 [\text{Nm}] = 1.05M_l + 11.3$ (Hainzl and Fischer, 2002; Horálek et al., 2002), which is a local modification of general moment-magnitude relation – see e.g. Hanks and Kanamori (1979). Note, that Fischer and Horálek (2005) supposed stress drop $\Delta\sigma$ of 10 MPa in the quoted study. Our results are presented in Figure 6 and summarized in Table 3, from where it is clear, that there is a good agreement between formula given by Fischer and Horálek and our results. The magnitude-radius relation can be further used e.g. for modelling the space-time swarm slip behaviour (Kolář et al., 2011).

We compared source radius versus seismic moment – Figure 7. The hypothesis of constant stress drop is a good approximation also for the W.B. events

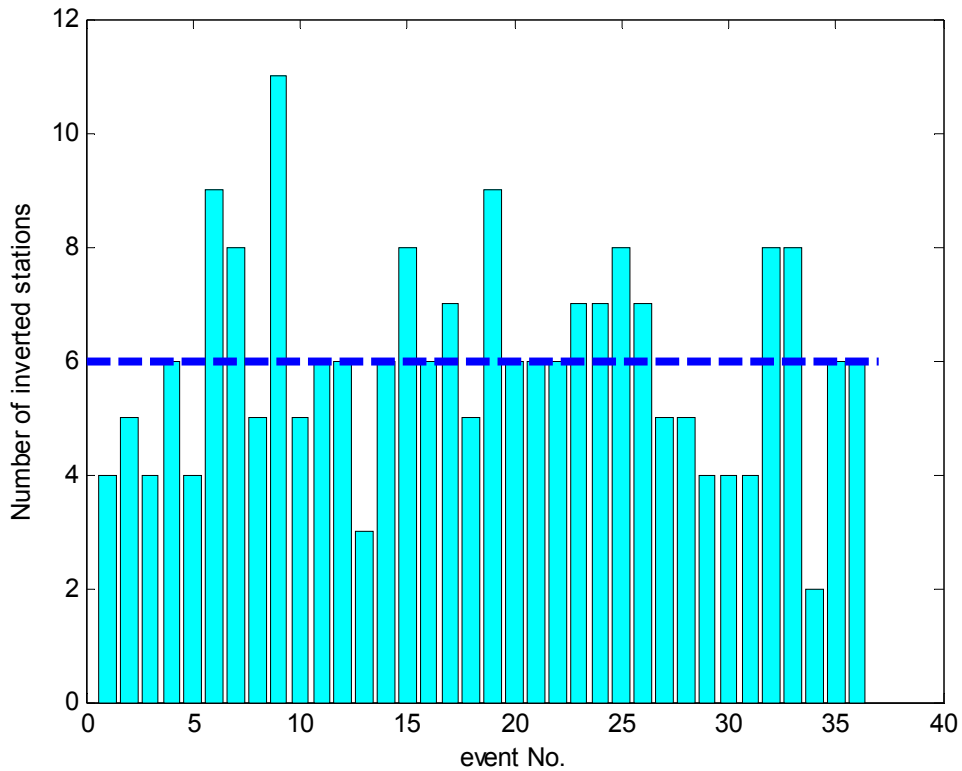


Fig. 5 Distribution of the observations: number of observations versus event number. Even if the inversion is fairly well over-determined (the average number of station for inversion is 6 – marked by dashed line), the azimuthal coverage is not quite favourable – c.f. Figure 4b.

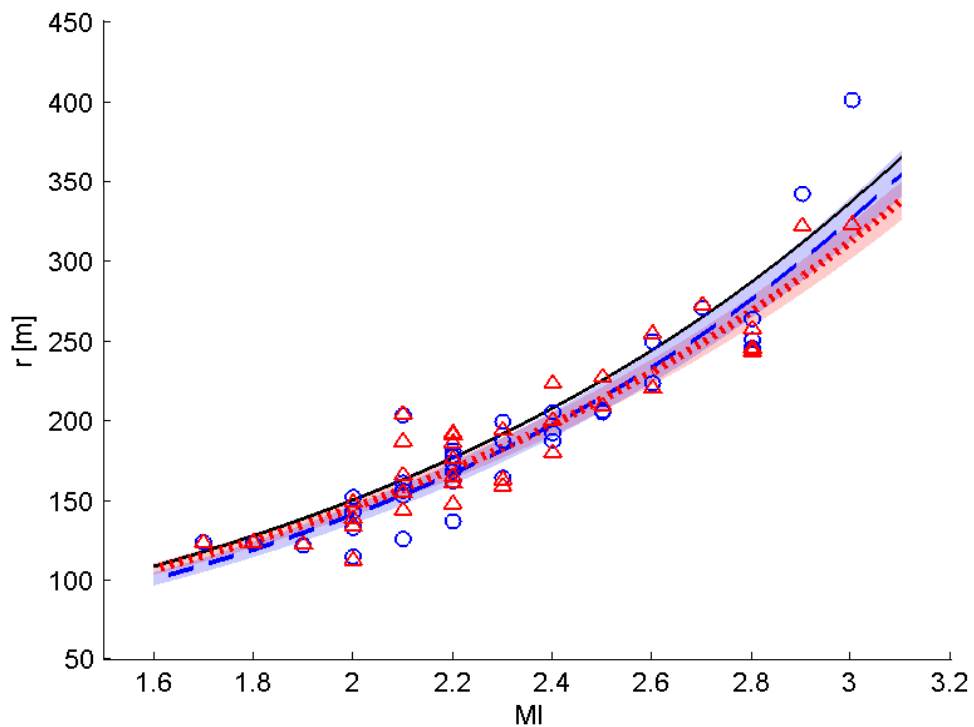


Fig. 6 Finite source radius versus magnitude: theoretical formula $r=30 \cdot 10^{(0.35 MI)}$ (Horálek and Fischer, 2005) is plotted by full line, the approximations from our inversion by dotted lines, their confidence intervals by coloured areas. Inversion results for circular source: 2 parameters inversion (circles and dashed line) and inversion with fixed v_r (i.e. 1 parameter inversion; triangles and dotted line).

Table 2 Result of the circular source model inversion.

Results of inversion: Event number (No.), number of stations included in particular inversion, source radius (r_1) and its error (inversion with fixed value of $v_r=0.85$) and source radius (r_2) and its error and rupture velocity (v_r) and its error.

No.	number of stations	r_1 [m]	r_1 error [m]	r_2 [m]	r_2 error [m]	v_{r2}	v_{r2} error
1	4	113	7	115	8	0.68	0.05
2	5	243	17	250	17	0.87	0.01
3	4	194	8	187	8	0.75	0.05
4	6	244	8	244	9	0.84	0.03
5	4	149	9	152	10	0.79	0.04
6	9	180	4	187	5	0.83	0.03
7	8	124	5	123	5	0.81	0.02
8	5	165	6	162	7	0.74	0.03
9	11	209	3	205	3	0.88	0.01
10	5	155	9	153	9	0.89	0.04
11	6	227	9	206	10	0.81	0.03
12	6	200	10	192	11	0.97	0.03
13	3	159	18	199	21	1.00	0.05
14	6	139	10	143	11	0.85	0.03
15	8	124	5	124	5	0.69	0.02
16	6	187	9	161	9	0.90	0.03
17	7	148	6	137	6	0.80	0.03
18	5	191	7	168	8	0.90	0.06
19	5	321	6	315	7	0.92	0.03
20	6	134	5	133	5	0.83	0.04
21	6	123	5	122	5	0.85	0.03
22	6	176	6	177	7	0.88	0.05
23	7	144	5	156	5	0.74	0.02
24	7	220	6	223	8	0.80	0.05
25	8	204	7	203	8	0.93	0.03
26	7	254	11	249	12	0.96	0.01
27	5	257	4	245	5	0.72	0.03
28	5	272	10	270	12	0.86	0.05
29	4	245	19	263	24	0.84	0.10
30	5	322	17	307	21	0.87	0.06
31	4	166	8	126	9	0.66	0.03
32	8	161	7	173	7	0.96	0.02
33	8	163	10	164	10	0.76	0.02
34	4	223	25	205	29	0.78	0.08
35	6	192	11	178	12	1.00	0.02
36	6	186	10	181	11	0.81	0.05

(c.f. Fig. 13 by Imanishi et al., 2004). The results correspond to the general worldwide stress drop relation, see e.g. comparative study of Kwiatek et al., (2011), however the details of the relation as well as its geographical limitation are still under the discussion. Our results show that in the W.B. region the stress drop ranges between 1 – 10 MPa with the

most frequent value $\Delta\sigma = 2.4$ MPa. This is in a good agreement with value $\Delta\sigma = 1.7$ MPa, given by Hainzl and Fischer (2002), who were investigating the 1997 swarm and compared spatial extent of the swarm activity with the fracture area of tectonic earthquakes (approach designed by Mai and Beroza, 2000).

We compared magnitude versus rupture velocity v_r . There is no significant relation between these two values – see Figure 8 (and c.f. Fig. 14 by Imanishi et al., 2004).

We conclude that (except the above mentioned magnitude versus source radius relation and the confirmation of a constant stress drop assumption) any studied relations between finite source parameters and other earthquakes characteristic show no (significant) correlation. This fact is in agreement with results given by Imanishi et al. (2004).

6. CONCLUSIONS

We determined parameters of circular finite source models for 36 West Bohemian events from earthquake swarm that took place in year 2000. The model was described by 2 parameters (source radius and rupture velocity), or optionally only by the source radius, when the value of rupture velocity was fixed. The extension from two-parameters model to four-parameters model (elliptical source) was found to be statistically insignificant and the circular source models can be considered as a good approximation of the studied events. But it could be also a consequence of lower reliability of results due to more complex models, which is caused by unfavourable azimuthal station coverage of the investigated events. Our results confirm the validity of theoretical relation between event magnitude M_l and source radius: $r=30*10^{(0.35 M_l)}$. Stopping phases method enables to invert data (delay of stopping phases) directly for the source parameter(s) without any need to suppose particular values of stress drop. On the contrary, the stress drop of processed events can be estimated afterwards. The set of studied events fairly well fits the theoretical assumption of a constant stress drop; it ranges between 1-10 MPa in our case with typical value 2.4 MPa. Such value is smaller than generally considered value (typically 10 MPa) however it is in agreement with value 1.7 MPa given by Hainzl and Fischer (2002). The smaller stress drop can be a consequence of the swarm nature of investigated events.

Any other studied relations between physical parameters did not yield any correlations, however such results are in agreement with other works (c.f. Imanishi et al., 2004). The method can be also applied to other data sets. Data from W.B. 2008 earthquake swarm with better station coverage (Horálek et al., 2009; Fischer et al., 2010) seem to be promising from this point of view. Another way concerning future data processing could be application of higher order seismic moment tensor formalism (Adamová and Šílený, 2010), which could possibly yield independent test of obtained finite source models.

Table 3 Values of constants and their errors in M_l versus source radius relation.

The relation is supposed in the form of $r=C_1*10^{(C_2 * M_l)}$. The errors were estimated during regression. Results for all investigated source models and inversions (i.e. data presented in Table 2) and the values derived by Fischer and Horálek (2005) are included. In addition we give also values derived from results given by Imanishi et al. (2004). Circular source equivalent of elliptic source model is achieved by converting elliptic source into circular one in such a way that the source area is preserved.

Region	Data	C_1 [m]	C_1 error [m]	C_2	C_2 error
W.B.	Values of C_1 and C_2 given by Fischer and Horálek (2005)	30		0.33	
W.B.	Present study				
	Circular source with fixed v_r (Table 2)	31.6	1.0	0.332	0.001
W.B.	Present study				
	Circular source with determined r and v_r (Table 2)	26.5	1.0	0.363	0.001
Western Nagano Japan	Elliptic source Imianishi et al. (2004)	12.0	1.2	0.463	0.019
Western Nagano Japan	Circular source equivalent Imanshi et al. (2004)	8.7	1.1	0.425	0.016

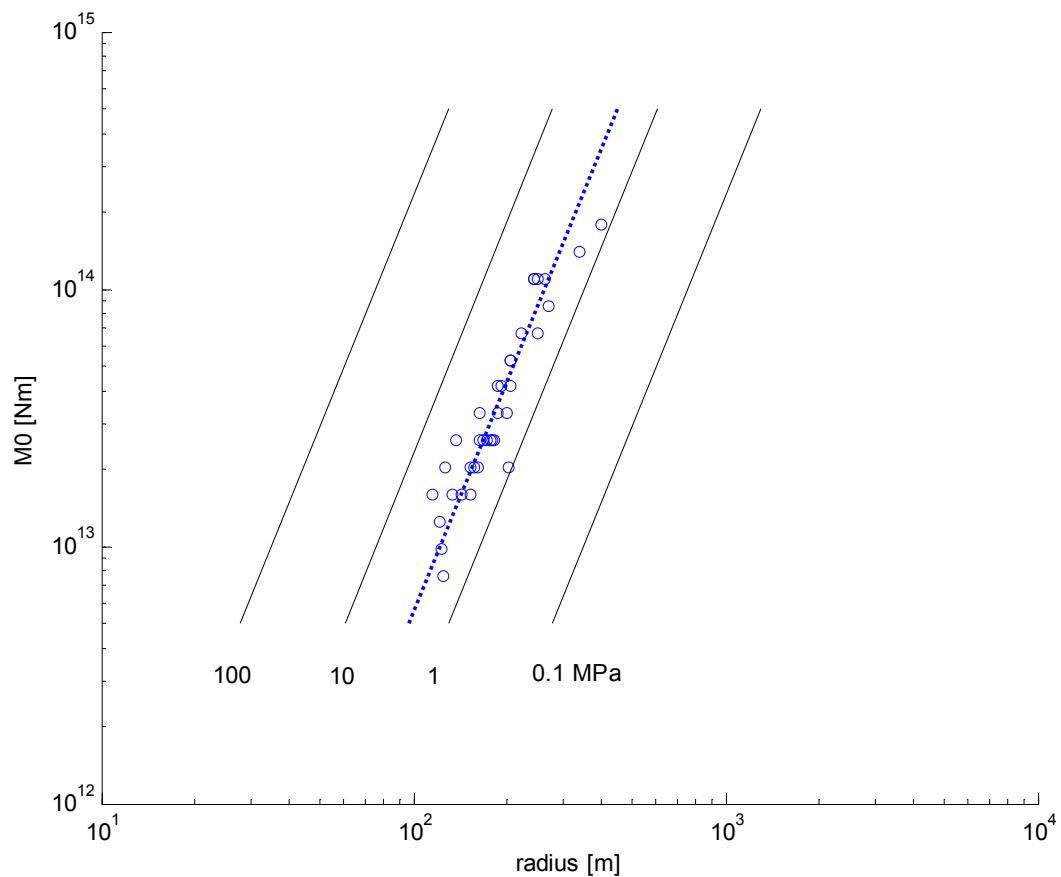


Fig. 7 Seismic moment M_0 (determined by relation $\log M_0 = 1.05M_l + 11.3$; Hainzl and Fischer, 2002; Horálek et al., 2002) versus source radius. Constant stress drop lines are plotted (full lines). The figure confirms constant stress drop assumption, all the values lie between values 1-10 MPa, with median 2.4 MPa (dotted line).

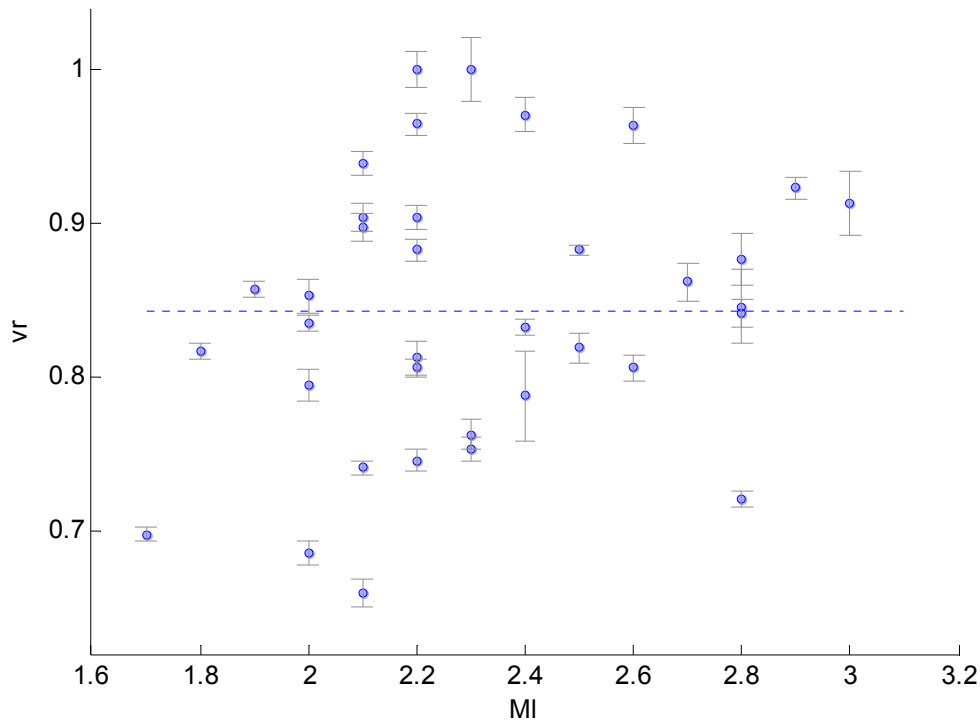


Fig. 8 Comparison of event magnitude versus rupture velocity v_r . There are plotted values of v_r (dots) and their error (values given in Table 2) - the average value of $v_r=0.85$ is plotted by dashed line. Even if some small upward trend can be possibly speculated, we consider such dependency as insignificant in the present case.

ACKNOWLEDGEMENT

We are thankful to WEBNET staff (coordinated by J. Horálek), namely to T. Fischer for his kind providing of selected seismograms of processed events and to (Ms.) A. Boušková for her providing of bulletin data. We are thankful to two unknown reviewers for numerous and constructive comments to the text.

The work was supported by the grant IAA300120805 (P. Kolář) of the Grant Agency of Acad. of Sci. of the Czech Republic; finalisation of the paper then by grant P210/10/1728 (Ms. Z. Jechumtálová) of the Grant Agency of the Czech Republic. Maps were prepared using the GMT software (Wessel and Smith, 1991).

REFERENCES

- Adamová, P. and Šílený, J.: 2010, Non-double-couple earthquake mechanism as an artifact of the point-source approach applied to a finite-extent focus. *Bull. Seism. Soc. Am.*, 100: 447–57.
- Aki, K. and Richards, P.G.: 1980, *Quantitative Seismology*. W. H. Freeman and Co., San Francisco.
- Beresnev, I.A. and Atkinson, G.M.: 1998, FINSIM – a FORTRAN Program for Simulating Stochastic Acceleration Time Histories from Finite Faults. *Seism. Res. Lett.* 69, 1, 27–32.
- Boender, C.G.E., Rinnooy Kan, A.H.G. and Timmer, G.T.: 1982, A Stochastic method for global optimisation. *Mathematical programming*, 22, 125–140.
- Bernard, P. and Madariaga, R.: 1984, A new asymptotic method for the modeling of near-field accelerograms. *Bull. Seism. Soc. Am.*, 74, 539–557.
- Boatwright, J.: 1980, A spectral theory for circular seismic sources: Simple estimates of source dimension dynamic stress drop, and radiated seismic energy. *Bull. Seis. Soc. Am.*, 70, 1–27.
- Brune, J.N.: 1970, Tectonic stress and the spectra of seismic shear waves from earthquakes. *J. Geophys. Res.*, 75, 4997–5009.
- Csendes, T.: 1988, Nonlinear parameter estimation by global optimization – Efficiency and reliability. *Acta Cybernetica*, VIII/4, 361–370.
- Fischer, T.: 2003, The August–December 2000 earthquake swarm in NW Bohemia: the first results based on automatic processing of seismograms. *J. Geodyn.*, 35, 59–81.
- Fischer, T.: 2005, Modeling of multiple-events using empirical Greens functions: method, application to swarm earthquakes and implications for their rupture propagation. *Geophys. J. Int.*, 163, 991–1005, doi:10.1111/j.1365-246X.2005.02739.x.
- Fischer, T. and Horálek, J.: 2005, Slip-generated patterns of swarm microearthquakes from West Bohemia/Vogtland (central Europe): Evidence of their triggering mechanism? *J. Geophys. Res.*, 110, B05S0X, doi: 10.1029/2004JB003363.

- Fischer, T., Horálek, J., Michálek, J. and Boušková, A.: 2010, The 2008 West Bohemia earthquake swarm in the light of the WEBNET network. *J. Seismol.*, 14, 4, 665–682, doi:10.1007/s10950-010-9189-4.
- Gaždová, R., Novotný, O., Málek, J., Valenta, J., Brož, M. and Kolínský P.: 2011, Groundwater level variations in the seismically active region of Western Bohemia in the years 2005-2010, *Acta Geodyn. Geomater.*, 8, 1, 17–27.
http://www.irsm.cas.cz/abstracts/AGG/01_11/2_Gazdova.pdf
- Hainzl, S. and Fischer, T.: 2002, Indications for a successively triggered rupture growth underlying the 2000 earthquake swarm in Vogtland/NW Bohemia. *J. Geophys. Res.*, 107(B12), 2338, doi:10.1029/2002JB001865.
- Hanks, T.C. and Kanamori, H.: 1979, A moment magnitude scale. *J. Geophys. Res.*, 84, 2348–2350.
- Horálek, J., Šílený, J. and Fischer, T.: 2002, Moment tensors of the January 1997 earthquake swarm in West Bohemia (Czech Republic): Double-couple vs. non-double-couple events, *Tectonophysics*, 356, 65–85.
- Horálek, J., Fischer, T., Boušková, A., Michálek, J. and Hrubcová, P.: 2009, The West Bohemian 2008-earthquake swarm: When, where, what size and data. *Studia Geophys. Geodet.*, 53 (3), 351–358.
- Ihmlé, P.F. and Ruegg, J.-C.: 1997, Source tomography by simulated annealing using broad-band surface waves and geodetic data: application to the Mw=8.1 Chile 1995 event. *Geophys. J. Int.*, 131, 146–158.
- Imanishi, K. and Takeo, M.: 1998, Estimates of fault dimensions for small earthquakes using stopping phases. *Geophys. J. L et.*, 25, 15, 2987–2900.
- Imanishi, K. and Takeo, M.: 2002, An inversion method to analyze rupture process of small earthquakes using stopping phases, *J. Geophys. Res.*, 107, B3.
- Imanishi, K., Takeo, M., Ellsworth, W.L., Ito, H., Matsuzawa, T., Kuwahara, Y., Iio, Y., Horiuchi, S. and Ohmi, S.: 2004, Source parameters and rupture velocities of microearthquakes in Western Nagano, Japan, determined using stopping phases. *Bull. Seis. Soc. Am.*, 94, 5, 1762–1780, doi: 10.1785/012003085.
- Lay, T. and Wallace, T.: 1995, *Modern Global Seismology*, Academic press, San Diego.
- Kolář, P.: 2003, Seismic source model from West Bohemia seismograms inversion - the method and preliminary results for ML2.0, Jan 17 1997 event. *Acta Montana*, 22 (129), ser. A, 33–49.
- Kolář, P.: 2010, Some possible correlations between electromagnetic emission and seismic activity during West Bohemia 2008 earthquake swarm, *Solid Earth*, 1, 93–98, doi:10.5194/se-1-93-2010, <http://www.solid-earth.net/1/93/2010/se-1-93-2010.html>
- Kolář, P.: 2011, A tool for determination of finite seismic source parameters via stopping phases method, in *Technical Computing Prague 2011*, pp. 69, <http://www.humusoft.com/akce/matlab11/sbornik/>
- Kolář, P., Růžek, B., Boušková, A. and Horálek, J.: 2011, Visualization of the fault slip connected with the West Bohemia earthquake swarms, *Acta Geodyn. Geomater.*, 8, 2 (162), 169-187, http://www.irsm.cas.cz/abstracts/AGG/02_11/7_Kolar.pdf
- Kwiątek, G., Plenkers, K., Dresen, G. and JAGUAR Research Group: 2011, Source parameters of picoseismicity recorded at Mponeng deep gold mine, South Africa: Implication for scaling relations. *Bull. Seis. Soc. Am.*, 101, 6, 2592–2608, doi: 10.1785/0120110094
- Madariaga, R.: 1976, Dynamics of an expanding circular fault, *Bull. Seis. Soc. Am.*, 66, 639–666.
- Mai, P.M. and Beroza, G.C.: 2000, Source scaling properties from finite-fault-rupture models. *Bull. Seis. Soc. Am.*, 90, 604–615.
- Menke, W.: 1989, *Geophysical data analysis: Discrete inverse theory*. Int. Geoph. Series, 45, Academic Press, Inc.
- Miller, J.: 1989, *Statistics for advanced level* (second edition), Cambridge, University press,
- Plicka, V. and Zahradník, J.: 2002, The use of eGf method for dissimilar focal mechanisms: The Athens 1999 earthquake, *Tectonophysics*, 359, 81–95.
- Press, H.W., Teukolsky, S.A., Vetterling, W.T. and Flannery, B.P.: 1992, *Numerical Recipes in C* (second edition), Cambridge, University press.
- Rao, J.N.K. and Shao, J.: 1992, Jackknife variance estimation with survey data under hot deck imputations. *Biometrica*, 79, 4, 811–822.
- Schenk, V. and Schenková, Z.: 2011, Horizontal strain, ³He/⁴He ration and intra-plate earthquake swarms. *Acta Geodyn. Geomater.*, 8, 3 (163), 303–308, http://www.irsm.cas.cz/abstracts/AGG/03_11/11_Schenkovi.pdf
- Stein, S. and Wysession, M.: 2003, *An introduction to Seismology, Earthquakes and Earth Structure*, Blackwell Publishing, Malden.
- Studia Geophysica et Geodetica*: 2000, (special issue devotes to West Bohemia topics): 44, 2–3.
- Studia Geophysica et Geodetica*: 2008, (special issue devotes to West Bohemia topics – Part 1): 52, 4.
- Studia Geophysica et Geodetica*: 2009, (special issue devotes to West Bohemia topics – Part 2): 53, 3.
- Štrunc, J. and Brož, M.: 2011, The detection of weak earthquakes in the Western Bohemia swarm area through the deployment of seismic arrays. *Acta Geodyn. Geomater.*, 8, 4 (164), 469-477, http://www.irsm.cas.cz/abstracts/AGG/04_11/8_Strunc.pdf
- Tichlaar, B.W. and Ruff, L.J.: 1989, How good are our best models? Jackknifing, bootstrapping, and earthquake depth. *EOS Trans. AGU*, 16, 593.
- Wessel, P. and Smith, W.H.F.: 1991, Free software helps map and display data. *EOS Trans. AGU*, 441, 72.
- wwwBRST: 2012, http://en.wikipedia.org/wiki/BRST_algorithm access: 25 May 2012.
- wwwWEBNET: 2012, <http://www.ig.cas.cz/en/structure/observatories/west-bohemia-seismic-network-webnet/> access: 25 May 2012.